

A large time increment method applied to an interface cohesive crack growing in compression-shear conditions

*Original*

A large time increment method applied to an interface cohesive crack growing in compression-shear conditions / Valente, Silvio; Alberto, Andrea; Barpi, Fabrizio. - In: ENGINEERING FRACTURE MECHANICS. - ISSN 0013-7944. - (2018). [10.1016/j.engfracmech.2016.04.019]

*Availability:*

This version is available at: 11583/2653255 since: 2016-10-17T14:03:20Z

*Publisher:*

Elsevier Science Limited

*Published*

DOI:10.1016/j.engfracmech.2016.04.019

*Terms of use:*

This article is made available under terms and conditions as specified in the corresponding bibliographic description in the repository

*Publisher copyright*

Elsevier postprint/Author's Accepted Manuscript

© 2018. This manuscript version is made available under the CC-BY-NC-ND 4.0 license  
<http://creativecommons.org/licenses/by-nc-nd/4.0/>. The final authenticated version is available online at:  
<http://dx.doi.org/10.1016/j.engfracmech.2016.04.019>

(Article begins on next page)

## Accepted Manuscript

A large time increment method applied to an interface cohesive crack growing in compression-shear conditions

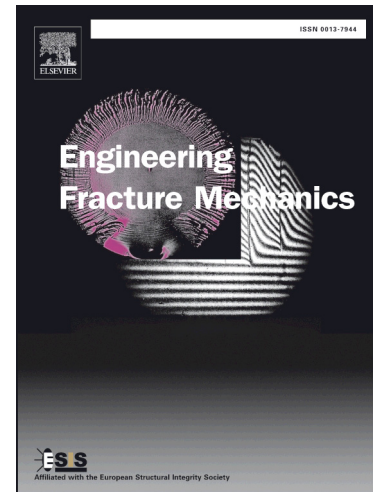
Silvio Valente, Andrea Alberto, Fabrizio Barpi

PII: S0013-7944(16)30175-8

DOI: <http://dx.doi.org/10.1016/j.engfracmech.2016.04.019>

Reference: EFM 5164

To appear in: *Engineering Fracture Mechanics*



Please cite this article as: Valente, S., Alberto, A., Barpi, F., A large time increment method applied to an interface cohesive crack growing in compression-shear conditions, *Engineering Fracture Mechanics* (2016), doi: <http://dx.doi.org/10.1016/j.engfracmech.2016.04.019>

This is a PDF file of an unedited manuscript that has been accepted for publication. As a service to our customers we are providing this early version of the manuscript. The manuscript will undergo copyediting, typesetting, and review of the resulting proof before it is published in its final form. Please note that during the production process errors may be discovered which could affect the content, and all legal disclaimers that apply to the journal pertain.

# A large time increment method applied to an interface cohesive crack growing in compression-shear conditions

Silvio Valente<sup>a,\*</sup>, Andrea Alberto<sup>a</sup>, Fabrizio Barpi<sup>a</sup>

<sup>a</sup>*Dep. of Structural, Geotechnical and Building Engineering, Politecnico di Torino,  
Corso Duca degli Abruzzi, 24, 10129 Torino, Italy*

---

## Abstract

When the long-time behaviour of a concrete dam is analysed, the International Commission of Large Dams recommends to neglect the tensile strength of the dam-foundation joint and to include the uplift pressure due to the water penetrating into the crack. In this context a non-linear problem of contact with friction occurs in the vicinity of the point which separates the damaged part of the joint from the undamaged one. In these conditions the solution depends on the stress path followed during the quasi-static incremental process. Therefore the classical Newton-Raphson fails to converge and has to be replaced by a Large Time Increment method. In this way it was possible to obtain realistic solutions for three different mechanical regimes.

### *Keywords:*

Cohesive crack model, concrete, hydro-mechanical coupling, interface crack, gravity dam

---

---

\*Corresponding author

*Email addresses:* [silvio.valente@polito.it](mailto:silvio.valente@polito.it) (Silvio Valente),  
[andrea.alberto@polito.it](mailto:andrea.alberto@polito.it) (Andrea Alberto), [fabrizio.barpi@polito.it](mailto:fabrizio.barpi@polito.it) (Fabrizio Barpi)

### Nomenclature

$c$	dam-foundation joint cohesion ( $\text{N/m}^2$ )
$h$	water level above the dam-foundation joint (m)
$h_{out}$	water level above the dam crest (m)
$H$	softening module ( $\text{N/m}^3$ )
$K_1, K_2$	stress intensity factors ( $\text{N/m}^{3/2}$ )
$P_{max}$	maximum value of the water pressure applied on the upstream edge ( $\text{N/m}^2$ )
$w_n$	normal component of the displacement discontinuity (m)
$w_t$	shear component of the displacement discontinuity (m)
$w$	effective value of the displacement discontinuity (m)
$w_c$	for $w > w_c$ the cohesive stress vanishes (m)
$w_{nc}$	for $w_n > w_{nc}$ the full water pressure is applied (m)
$\gamma$	specific weight of water ( $\text{N/m}^3$ )
$\phi$	friction angle applied to the dam-foundation joint
$\sigma_n$	pressure applied to the dam-foundation joint ( $\text{N/m}^2$ )
$\tau$	shear stress applied to the dam-foundation joint ( $\text{N/m}^2$ )
$\tau_p$	max value of shear stress applied to the FCT ( $\text{N/m}^2$ )
$\tau_r$	residual value of the shear stress applied to the dam-foundation joint ( $w > w_c$ ) ( $\text{N/m}^2$ )
COD	Crack Opening Displacement, $w_n$ (m)
CSD	Crack Sliding Displacement, $w_t$ (m)
FCT	Fictitious Crack Tip. Point between damaged and undamaged part of the joint
FPZ	Fracture Process Zone, where the non-linear phenomena are localized.

## 1. Introduction

In dam engineering it is often necessary to model a closed crack growing in shear conditions. This is for example the case of the quasi static analysis of a crack growing at the interface between a gravity dam and the rock foundation. In this case, since the crack starts at the upstream edge of the dam, the water can penetrate and wash away the smallest aggregates of the concrete. This phenomenon can be considered as a corrosion which reduces the resisting material properties compared to the same properties measured during a short-time laboratory test. Looking at the long-time behaviour of the structure, the International Commission of Large Dams (shortened ICOLD, see [1]) recommends to neglect the tensile strength of the joint. In what follows, in order to remember that the numerical analysis is based on a reduced set of resisting properties, the term subcritical crack propagation is used.

After this preliminary remarks, following the terminology of the cohesive crack model, it is possible to observe that a shear displacement discontinuity (Crack Sliding Displacement, shortened CSD) starts growing at a point, called Fictitious Crack Tip (shortened FCT), which is still subjected to a compression stress (see Fig. 1). The normal component of the displacement discontinuity (Crack Opening Displacement, shortened COD) will appear at the same point later on. Therefore the asymptotic expansion for a cohesive crack [2], [3], [4] or other techniques [5], [6], [7], [8], [9], [10], [11], [12], [13], [14], [15], [16] cannot be applied. Therefore the cohesive crack model has to be re-formulated with the focus on the shear stress component [17]. In this context the solution depends on the stress path followed during the quasi-static incremental process. Therefore the classical Newton-Raphson fails to converge and has to be replaced by a Large Time Increment Method [18], [19] described in the following sections.

## 2. The mechanical model

One of the main differences between a model related to a specimen tested in the laboratory and a model related to a large structure is due to the effects of the self-weight. The analysis of the gravity dam shown in Fig. 1 begins from an initial state, which is a static equilibrium configuration of the dam and of an appropriate portion of the rock foundation. The equilibrium state includes both horizontal and vertical stress components in both materials (concrete

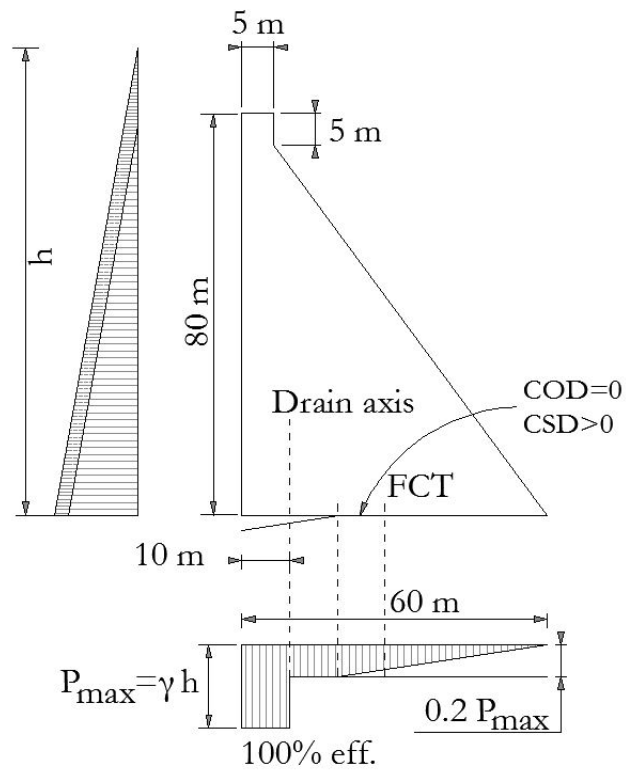


Figure 1: Gravity dam model proposed as a benchmark by ICOLD.

and rock). It is important to establish these initial conditions correctly so that the problem begins from an equilibrium state. In this initial state the reservoir is empty, the only load applied is the self-weight, the dam/rock contact is frictionless [20], the incremental solution is unique, the classical Newton-Raphson method converges and the interface is free from tangential stresses.

### 2.1. Traction-Separation law applied to the Fracture Process Zone

Once the equilibrium state is achieved in this initial phase, following the classical hypothesis of the cohesive crack model, a critical condition at the FCT is looked for. With reference to Fig. 1, the points on the right side of the FCT are tied, so that no displacement discontinuity can occur after this operation. With reference to the cohesive crack model, this portion of the interface plays the role of an undamaged ligament. On the contrary, the portion of the interface on the left side of the FCT is called Fracture Process Zone (shortened FPZ). All the non-linear phenomena occurring afterwards are localized into the FPZ. Concrete and rock outside the FPZ behave linearly.

This implementation of the cohesive crack model is based on two stages :

- a) a global one in which the FCT is moved ahead of one increment;
- b) a local one in which the non-linear conditions occurring in the FPZ are taken into account.

This two-stage approach is known in the literature as a Large Time Increment approach [18], [19]. The main consequences of this two-stage approach are:

- a) A previous converged load increment is not required.
- b) The iterations done during the local stage are characterized by displacement and stress fields which are not real. They are just a way to reach a critical condition at FCT and can be forgotten. In this case the node-to-segment friction contact problem is solved by means of the Lagrange multipliers [20].

Once the critical condition has been reached, it has to be saved and plotted as a step of the global stage, which has a clear physical meaning.

Since the model outside the process zone behaves linearly and includes a crack, a generic load increment occurring during the local stage can induce a singular stress increment at the FCT. The following two assumptions, related to the FPZ, prevent the onset of such a singular stress increment:

- a) as long as the FPZ is closed, the normal component of the displacement discontinuity vanishes, and therefore the stress intensity factor is  $K_1 = 0$ . In these conditions, following the Coulomb law (see Fig. 2) , the peak value of the tangential stress is :

$$\tau_p = c + \sigma_n \tan(\phi) \quad (1)$$

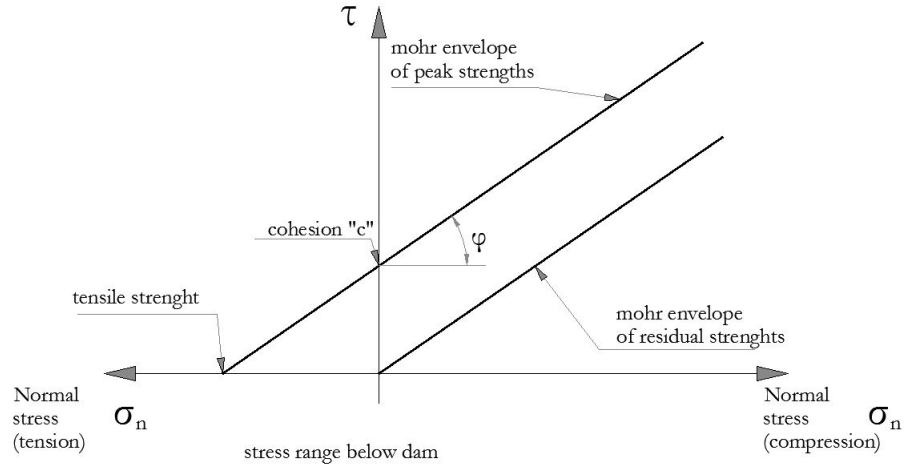


Figure 2: Mohr-Coulomb strength criterion on the interface.

- b) since a new step in the global stage starts only when the FCT is in critical conditions, since a rigid-plastic traction-separation law is assumed (Fig. 3), the stress intensity factor remains  $K_2 = 0$  during the iterations of the local stage.

The effective displacement discontinuity is assumed as:

$$w = \sqrt{w_n^2 + w_t^2} \quad (2)$$



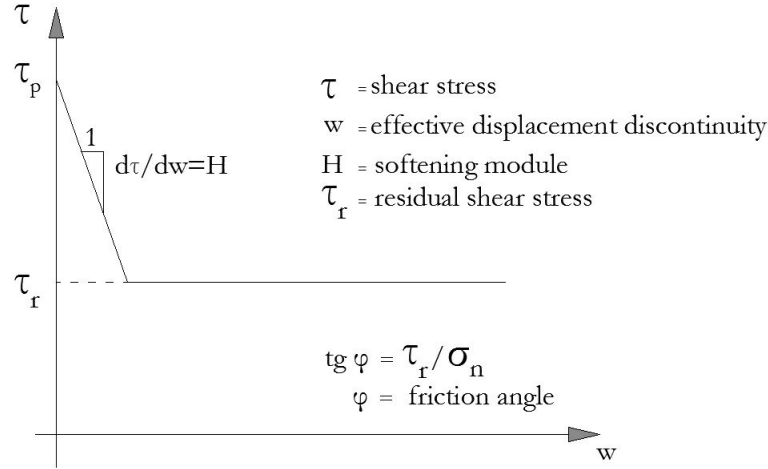


Figure 3: The rigid-softening cohesive law applied to the interface.

The value assumed for the joint properties  $c$ ,  $\phi$  and  $H$  are shown in Tab.

1. Tab. 2 shows the material properties.

Parameters	Unit	Value
Peak cohesion $c$	MPa	0.7
Residual cohesion	MPa	0
Tensile strength	MPa	0
Friction angle $\phi$	deg	30
Softening module $H$	MPa/mm	-0.7
Critical value $w_c = -c/H$	mm	1

Table 1: Properties of the concrete-rock interface.

## 2.2. Crack growth conditions in the closeness of the Fictitious Crack Tip

The above mentioned hypotheses are related to a surface: the dam-to-foundation interface. On the contrary, the following hypotheses are related to a volume of dam concrete and a volume of rock foundation. Since the expected strain field is smooth, special tip elements are not used. Both

domains are meshed by means of triangular elements of constant strain type. As shown in Figg. 4 and 5, the dam is divided into 2205 elements and the foundation into 5673 elements. In the closeness of the interface, the triangles are assumed as equilateral, with a side of 0.06 m. Figg. 8, 9, 10 show that this size is sufficiently small to obtain that the FPZ is always divided into 6 elements at least. The four stress components are computed in two elements connected to the joint and to the FCT: one for the dam and another for the foundation. The stress level is compared to the Mohr-Coulomb criterion shown in Fig. 2.

### 2.3. The hydro-mechanical coupling hypothesis

Fig. 1 shows the assumed distribution of uplift pressure in the case of complete drain efficiency. The pressure is assumed constant up to the point where the crack opening displacement is larger than a threshold value of  $w_{nc} = 10^{-6}$  m. Elsewhere the pressure is a linear function of the position, vanishing at the downstream edge.

Parameters	Unit	Rock	Concrete
Young module	MPa	41000	24000
Poisson ratio	-	0.10	0.15
Tensile strength	MPa	2.6	1.3

Table 2: Properties of rock and concrete.

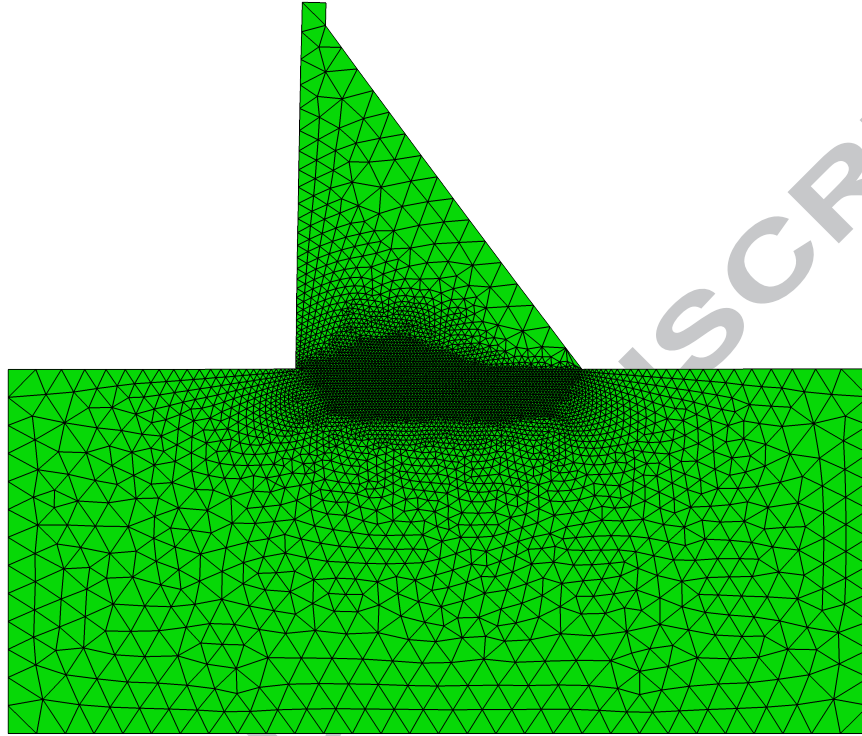


Figure 4: The Finite element mesh used.

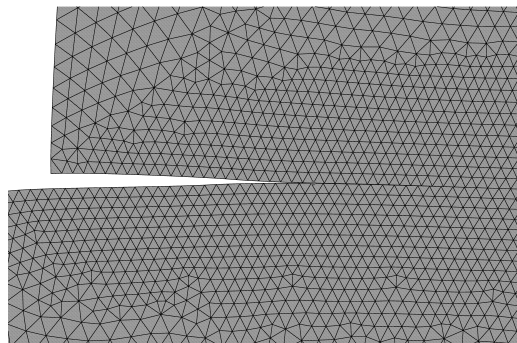


Figure 5: Deformed mesh for FCT position 24 m; displacements enlarged 700 times.

#### 2.4. The frictional contact model

Since both materials are discretized by means of linear elements, in the node-to-segment contact problem, the slide line segment is linear, too. In the frictional contact problem it is necessary to determine whether a node sticks or slips. To solve this problem the following tests are used. If the node is currently sticking, it is checked whether the magnitude of the frictional stress exceeds the critical value. Hence, if it is:

$$\tau > c(w) + \sigma_n \tan(\phi) \quad (3)$$

the state is changed to slipping. If the node is slipping, the direction of slipping is compared with the frictional stress applied at the start of the iteration. If, at the end of the iteration, it is:

$$\tau \dot{w}_t < 0 \quad (4)$$

the state is changed to sticking (a dot denotes the time derivative). The above mentioned conditions are applied through a Lagrange multipliers formulation (see [20]).

During the Newton-Raphson process an alternate stick-to-slip or closed-to-open transition can prevent the convergence. Therefore a dual stage approach is used and each second stage starts just after the self weight application on a frictionless joint. The loading path is presented hereafter. The conventional time is assumed as  $T = 0$  when the reservoir is empty and  $T = 1$  when the water level reaches the dam crest. During this phase a proportional loading is assumed and  $T$  is the external load multiplier.

For  $T > 1$  the overtopping water level  $h_{ovt}$  plays the role of external load multiplier. In this case a uniform load distribution  $\gamma h_{ovt}$  is applied to the upstream edge.

For  $T < T_1$  all contact nodes are sticking and closed.

For  $T_1 < T < T_2$  only stick-to-slip transitions occur.

For  $T_2 < T < T_3$  both transitions (closed-to-open and stick-to-slip) occur.

In both cases ( $T \leq 1$  and  $T > 1$ ), the external load is increased monotonically, and the above mentioned transitions start at the upstream edge and move monotonically to the FCT, without reverting.

Since the displacements are large when compared to the segment length, a finite sliding formulation is applied.

Since the Coulomb's law of friction is included in the model, a non-symmetric solver is used.

As an example, Fig.6 shows the maximum value of a  $w_t$  increment computed during the local stage iterations when the distance of the FCT from the upstream edge is 18 m and the external load multiplier  $T$  is increase from 0.90 to 0.95. In this case both transitions occur. When the above mentioned distance is increased to 36 m, when  $h_{out}$  is increased from 0.4 to 0.8m more transitions occur as shown in Fig.7.

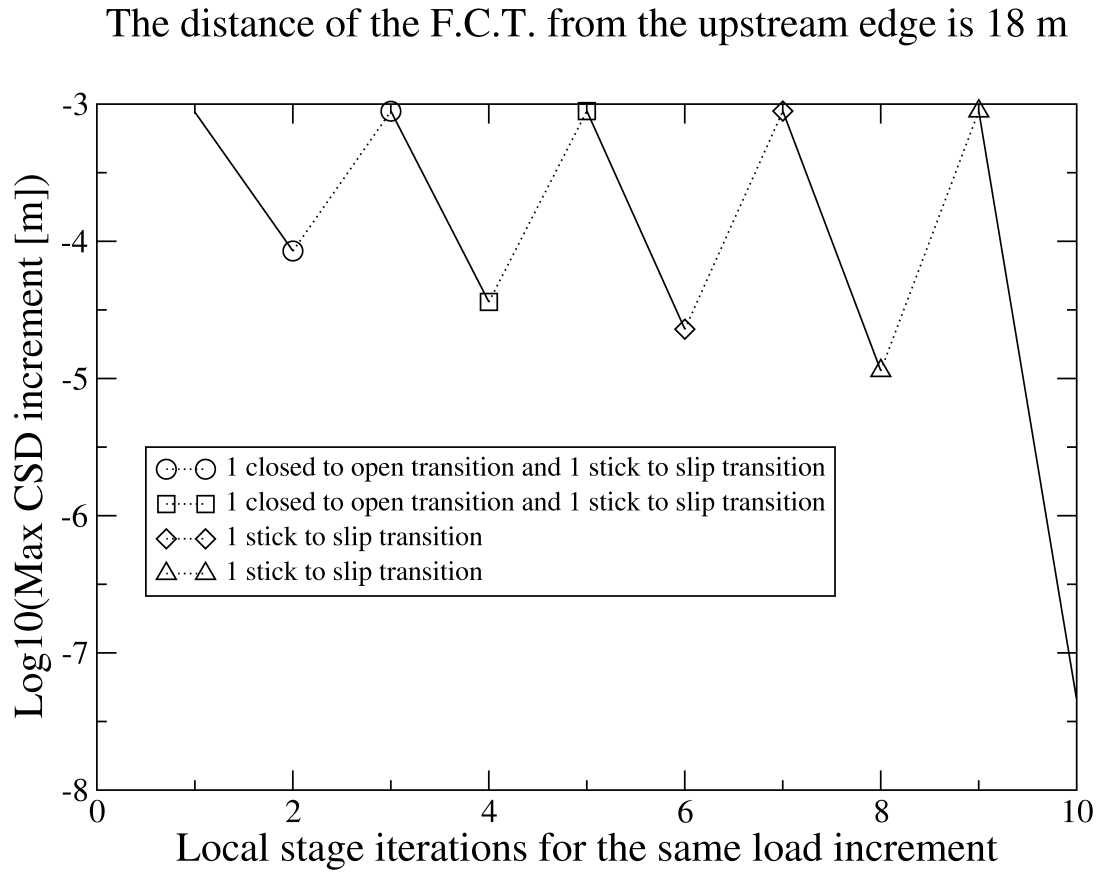


Figure 6: Local stage iterations when the external load multiplier  $T$  is increased from 0.90 to 0.95.

It is worthwhile noting that:

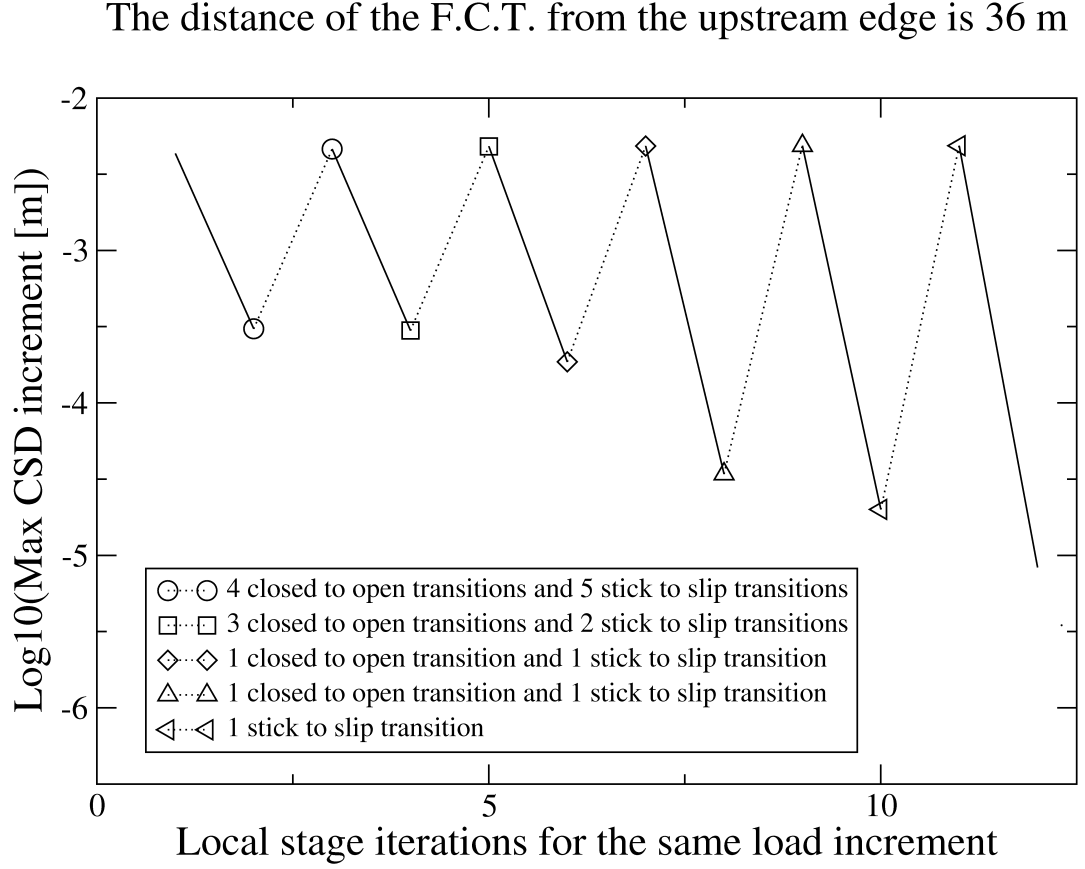


Figure 7: Local stage iterations when the external load multiplier  $h_{ovt}$  is increased from 0.4 to 0.8 m.

- each transition shown in Figg.6 and 7 induces an increment in the stress level occurring at FCT. When this level reaches the critical value shown in Fig. 2 the local stage ends.
- the friction angle  $\phi$  remain unchanged during the stick-to-slip transition.
- as long as the FCT moves towards the downstream edge the fraction of undamaged joint shrinks. As a consequence the increments of  $w_t$  and  $w_n$  become larger, as shown in Fig.7.

### 3. Results

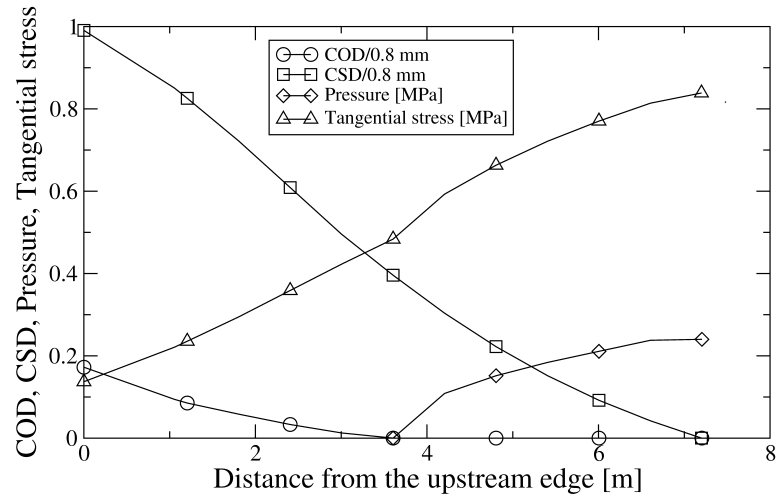
Fig. 8 shows the results at the end of the local stage when the distance of the FCT from the upstream edge is (a) 7.2 m. (b) 12 m.

Similarly, Figg. 9 and 10 refer to a distance respectively of 18,24,30 and 36 m.

It is possible to observe that the method applied is able to manage three different regimes:

- a) in Fig. 8a the FPZ is not completely developed ( $w < w_c$  everywhere),
- b) in Figg. 8b, 9, 10a, the point where the tangential cohesive stress vanishes is open. In other words, the condition  $w = w_c$  is achieved in a point where it is  $w_n > 0$  ( $w_c$  is shown in table 1),
- c) in Fig. 10a the point where the tangential cohesive stress vanishes is closed ( $\sigma_n > 0$ ). In other words, due to large  $w_t$  values, the condition  $w = w_c$  is achieved in a point where it is  $w_n = 0$ .

(a): Global step n.1: FCT position 7.2 m, load level 70% of full reservoir



(a): Global step n.1: FCT position 7.2 m, load level 70% of full reservoir

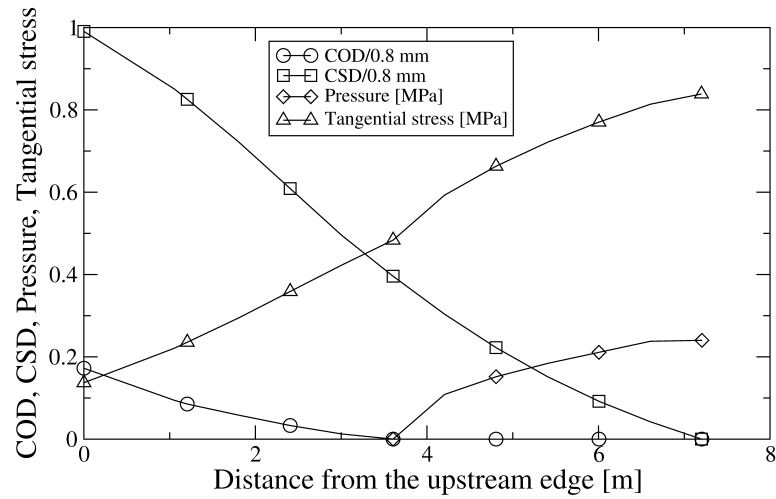
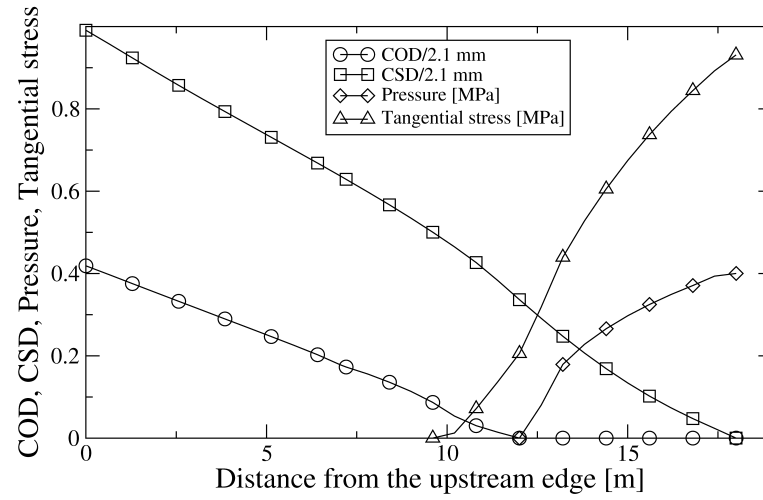


Figure 8: Results for the global stage step n.1(a) and n.2(b)



(a): Global step n.3: FCT position 18 m, load level 95% of full reservoir



(b): Global step n.4: FCT position 24 m, overtopping water level 0.08 m

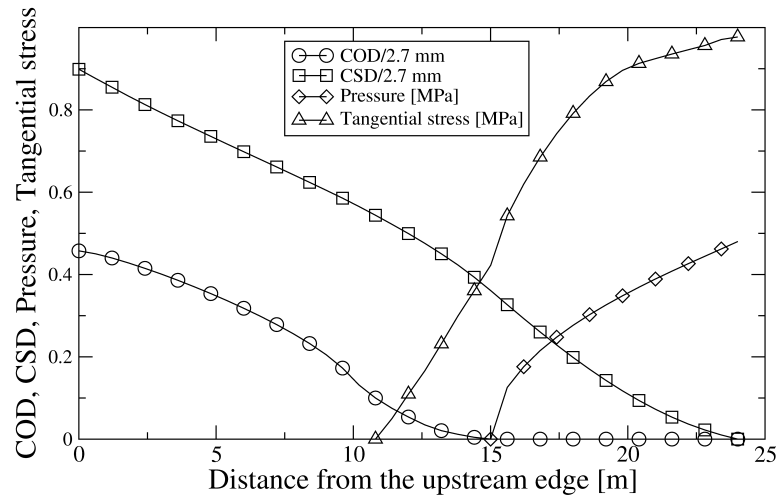
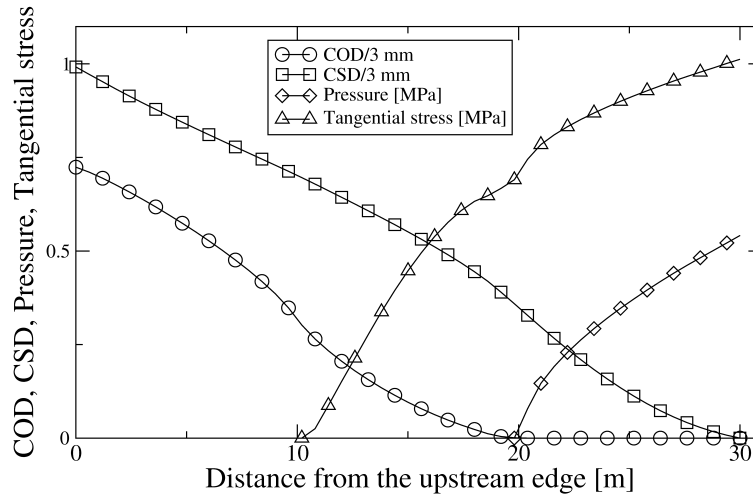


Figure 9: Results for the global stage step n.3(a) and n.4(b)

(a): Global step n.5: FCT position 30 m, overtopping water level 0.48 m



(b): Global step n.6: FCT position 36 m, overtopping water level 0.8 m

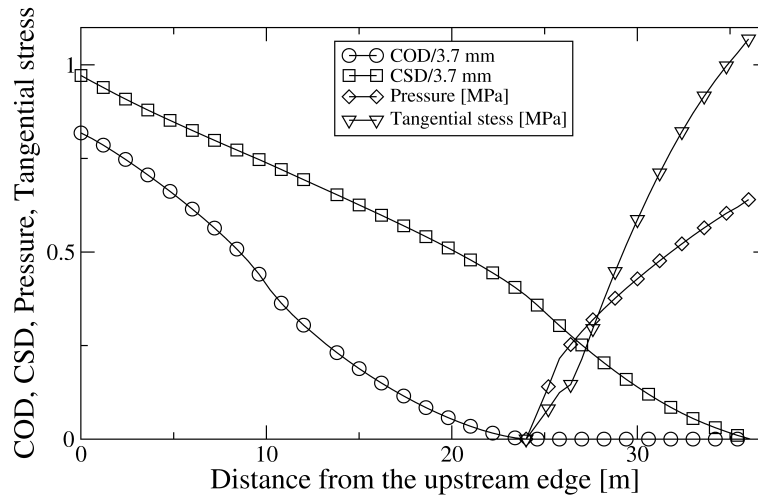


Figure 10: Results for the global stage step n.5(a) and n.6(b)

Fig. 11 shows the length of the compressed part of the FPZ as a monotonic increasing function of the FCT distance from the upstream edge. The tensile strength of the rock foundation (2.6 MPa) is enough to prevent a crack branching downwards.

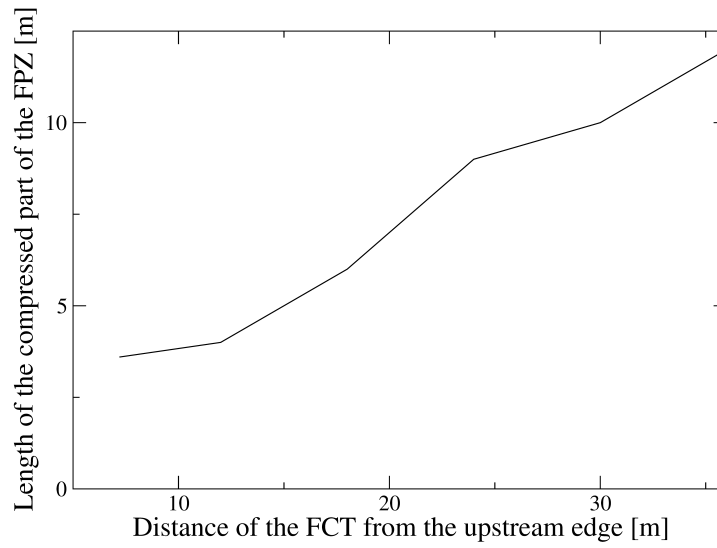


Figure 11: Length of the compressed part of the FPZ

Fig. 12 shows the water level evolution during the subcritical crack propagation.

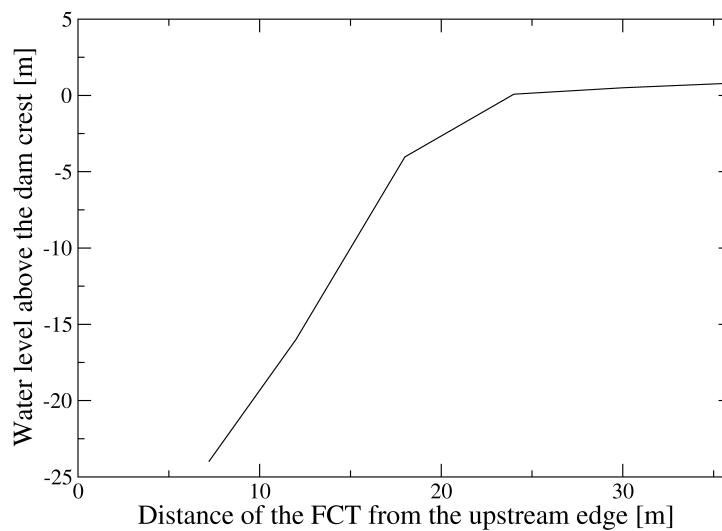


Figure 12: Water level above the dam crest during the subcritical crack propagation.

Fig. 13 shows the water penetration during the subcritical crack propagation.

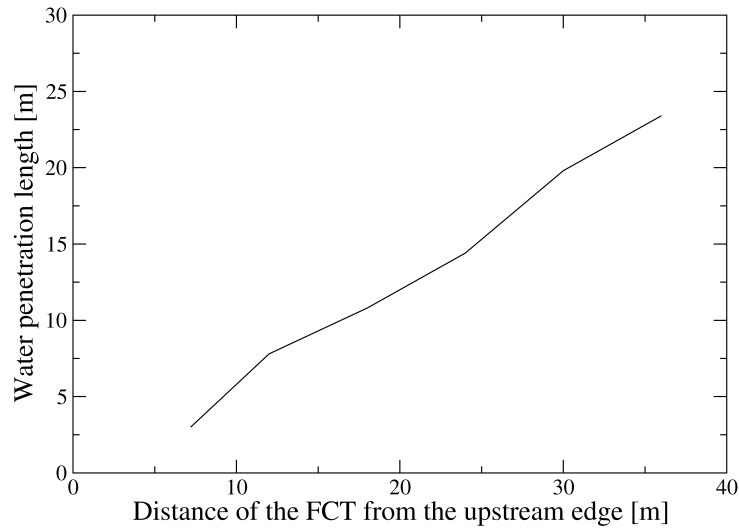


Figure 13: Water penetration during the subcritical crack propagation.

#### 4. Conclusions

- 1) The cohesive crack model can be used in the context of a large-scale engineering problem.
- 2) The uplift pressure induced by the water penetrating the open part of the crack can be taken into account.
- 3) The corrosion induced by the water penetrating the closed part of the crack can be taken into account through an appropriate reduction of the joint strength properties (subcritical crack propagation).
- 4) In this case the phenomenon cannot be modeled through a continuous sequence of load increments in the context of the Newton-Raphson method. On the contrary, it is necessary to divide the whole process in a sequence of LARGE Time INcrements (shortened LATIN). Therefore each large time increment can be simulated independently from the previous one.
- 5) This two-stage approach is able to model three different mechanical regimes occurring during the crack propagation process.

#### 5. References

##### References

- [1] ICOLD. Imminent failure flood for a concrete gravity dam. In *5th International Benchmark Workshop on Numerical Analysis of Dams*, Denver, CO, 1999.
- [2] B.L. Karihaloo and Q.Z. Xiao. Asymptotic fields at the tip of a cohesive crack. *International Journal of Fracture*, 150:55–74, 2008. doi: 10.1007/s10704-008-9218-2.
- [3] F. Barpi and S. Valente. The cohesive frictional crack model applied to the analysis of the dam-foundation joint. *Engineering Fracture Mechanics*, 77:2182–2191, 2010. ISSN: 0013-7944, doi: 10.1016/j.engfracmech.2010.02.030.
- [4] A. Alberto and S. Valente. Asymptotic fields at the tip of a cohesive frictional crack growing at the bi-material interface between a dam and the foundation rock. *Engineering Fracture Mechanics*, 108:135–144, 2013. ISSN: 0013-7944, doi: 10.1016/j.engfracmech.2013.05.005.

- [5] S. Valente. Bifurcation phenomena in cohesive crack propagation. *Computers and Structures*, 44(1/2):55–62, 1992.
- [6] F. Barpi and S. Valente. Modeling water penetration at dam-foundation joint. *Engineering Fracture Mechanics*, 75/3-4:629–642, 2008. doi: 10.1016/j.engfracmech.2007.02.008.
- [7] F. Barpi and S. Valente. Failure lifetime of concrete structures under creep and fracture. *Magazine of Concrete Research*, 63(5):371–376, 2011. ISSN: 00249831, doi: 10.1680/mac.9.00159.
- [8] F. Barpi and S. Valente. Lifetime evaluation of concrete structures under sustained post-peak loading. *Engineering Fracture Mechanics*, 72:2427–2443, 2005. doi:10.1016/j.engfracmech.2005.03.010.
- [9] S. Liamani, B.B.Bouiadjra, B.Serier, and M.Belhouari. Interaction effects between interfacial and sub-interfacial cracks in gravity dam. *Middle East Journal of Scientific Research*, 16(5):678–683, 2013. ISSN: 19909233, DOI: 10.5829/idosi.mejsr.2013.16.05.11057.
- [10] R. Serpieri, E. Sacco, and G. Alfano. A thermodynamically consistent derivation of a frictional-damage cohesive-zone model with different mode i and mode ii fracture energies. *European Journal of Mechanics A/Solids*, 49:13–25, 2015. ISSN: 09977538, doi: 10.1016/j.euromechsol.2014.06.006.
- [11] M.A. Hariri-Ardebili, H. Mirzabozorg, and M.R. Kianoush. Seismic analysis of high arch dams considering contraction-peripheral joints coupled effects. *Central European Journal of Engineering*, 3(3):549–564, 2013. ISSN: 18961541, DOI: 10.2478/s13531-013-0111-z.
- [12] G. Bolzon and G. Cocchetti. Direct assessment of structural resistance against pressurized fracture. *International Journal for Numerical and Analytical Methods in Geomechanics*, 27:353–378, 2003. ISSN: 03639061, doi:10.1002/nag.276.
- [13] F. Barpi and S. Valente. Size-effects induced bifurcation phenomena during multiple cohesive crack propagation. *International Journal of Solids and Structures*, 35(16):1851–1861, 1998. ISSN: 00207683.

- [14] F. Barpi and S. Valente. Fuzzy parameters analysis of time-dependent fracture of concrete dam models. *International Journal for Numerical and Analytical Methods in Geomechanics*, 26:1005–1027, 2002. doi: 10.1002/nag.235.
- [15] F. Barpi and S. Valente. A fractional order rate approach for modeling concrete structures subjected to creep and fracture. *International Journal of Solids and Structures*, 41/9-10:2607–2621, 2004. doi: 10.1016/j.ijsolstr.2003.12.025.
- [16] M. Shi, H. Zhong, E.T. Ooi, C. Zhang, and C. Song. Modeling of crack propagation of gravity dams by scaled boundary polygons and cohesive crack model. *International Journal of Fracture*, 183(1):29–48, 2013. doi: 10.1007/s10704-013-9873-9.
- [17] M. Castelli, A. Allodi, and C. Scavia. A numerical method for the study of shear band propagation in soft rocks. *International Journal for Numerical and Analytical Methods in Geomechanics*, 33:1561–1587, 2009. ISSN = 03639061, doi:10.1002/nag.778.
- [18] P. Ladeveze. *Nonlinear computational structural mechanics: new approaches and non-incremental methods of calculations*. Springer book, New York, 2012. ISBN=1461214327,9781461214328.
- [19] B. Vandoren, K. De Proft, A. Simone, and L. J. Sluys. A novel constrained large time increment method for modeling quasi-brittle failure. *Computer Methods in Applied Mechanics and Engineering*, 265:148–162, 2013. ISSN = 00457825, doi:10.1016/j.cma.2013.06.005.
- [20] P. Wriggers. *Computational contact mechanics*. Springer book, Germany, 2002. doi: 10.1007/978-3-540-32609-0.

## References



## HIGHLIGHTS

The corrosion induced by the water penetration reduces the joint strength properties.

The hydro-mechanical coupling can be taken into account.

The cohesive zone model can be used in the context of large scale engineering problems

The two-stage approach proposed is able to control three different mechanical regimes.